

***In silico* exploration of *Elaeocarpus ganitrus* extract phytochemicals on STAT3, to assess their anticancer potential**

Mehnaj¹, Abdul Roouf Bhat² and Fareeda Athar^{1*}

¹ Centre for Interdisciplinary Research in Basic Sciences, Jamia Millia Islamia, New Delhi-110025, India

² Department of Chemistry, Government Degree College, Baramulla-193101, India

* Corresponding author, E-mail: fathar@jmi.ac.in

Abstract

Elaeocarpus ganitrus Rox of the Elaeocarpaceae family is a broad-leaved medicinal plant and exhaustively used in orthodox systems of treating diseases. However, its anticancer impact and propensity to STAT3 has not yet been analyzed. The plant's extracts were *in vitro* assayed on the HeLa cell line and subsequently, GC-MS chromatogram of the methanolic, and chloroform extracts of the plant revealed that 106 compounds were present in the extracts. Subsequent filtration using Lipinski rules resulted in 81 phytochemicals being selected for the docking process with pre-selected receptor STAT3 (6NJS). Twenty-six out of 81 phyto-ligands showed high binding energy. Many drugs have weak pharmacokinetic properties and cellular toxicity and consequently, cannot pass through clinical trials. Hence, it is essential to determine the pharmacokinetic parameters of the phytoligands showing preferred binding with receptor 6NJS to consider the apparent bioavailability. The data for pharmacokinetics behavior, bioavailability extent, drug-likeness properties, medicinal chemistry friendliness, and toxicity of 26 phytochemicals with referenced inhibitors was explored. These 26 compounds were further checked for their ADMET properties by using the swissADME and PROTOX-II web server with the known inhibitors plumbagin and sanguinarine to determine the lead phytocompounds. The predictions of ADMET properties obtained six suitable phytocompounds (EG-9, EG-12, EG-13, EG-15, EG-16 and EG-26) of *E. ganitrus*, and found to be a perfect fit in the bioavailability radar. 2D and 3D interaction of phytoligands with the STAT3 show that the binding is through lys97, suggesting NH₂-terminal domain binding of STAT3 with ligands which is the main mono-ubiquitin conjugation spot. Most of the phytoligands interactions exist in the Linker domain and Transactivation domain of the STAT3.

Citation: Mehnaj, Bhat AR, Athar F. 2024. *In silico* exploration of *Elaeocarpus ganitrus* extract phytochemicals on STAT3, to assess their anticancer potential. *Medicinal Plant Biology* 3: e009 <https://doi.org/10.48130/mpb-0024-0010>

Introduction

Cancer is a cluster of diseases and STAT3 protein has significant roles in all types of cancer. Signal transducer and activator of transcription (STAT), belong to the family of cytoplasmic transcription factors, activate and transduce extracellular growth factor, and also affect cytokine signals and affect gene transcriptional events. STAT3 mutant intrinsically alone is enough to instigate oncogenic transformation, and tumorigenesis^[1–3]. A survey of the current literature reveals that STATs have transactivated domains and play a significant role in cancer migration and invasion. Hampering of c-Src kinase activity or downregulation of STAT3 signaling stimulates apoptosis^[4]. The study of chemical interactions between STAT3 receptor and phytochemicals assist in drug designing and hence in cancer therapy^[5]. There are a variety of phytochemicals that have a high propensity to modulate directly or indirectly the STAT3 signaling pathway. Triterpenoids like betulinic acid, polyphenols curcuminoids, plumbagin a naphthoquinone, diosgenin a steroid, hydroxycinnamic acid, and thymoquinone are the phytochemicals that suppress STAT3 expression^[6]. Many plant-derived phytochemicals manifest high anticancer activity and lead researchers to adopt integrated multifaceted research techniques^[7–11]. Though, *Elaeocarpus ganitrus* Roxb.

(also known as Rudraksha) constitutively placed in Ayurvedic system, also has anticancer potential^[12]. Recently its silver nanoparticle has been assessed for anticancer and antiproliferative activities^[13]. Its impact on STAT is yet to be explored. In the last few decades, phytochemical composition of *Elaeocarpus* genus has been extensively investigated. Phytochemicals of various extracts of different parts of the plant showed the presence of alkaloids, flavonoids, carbohydrates, glycosides, proteins, quinine, coumarins, tannins, minerals, vitamins, saponins, phenolic compounds, and fixed oils in a high concentration, thus adding to its medicinal value^[14]. The pharmacological screening of metabolites like polyphenols, alkaloids, terpenoids and flavonoids have been explored to demonstrate cancer pathways to ascertain possible mechanism^[15–18]. As stated in the literature, the beads and the bark of the plants have been extensively studied while the leaves of the *E. ganitrus* have not been studied for their anticancer efficiency. Besides, leaves of the plants were shown to have good antioxidant potential^[19,20]. The emphasis of the study is to identify phytochemicals retrieved from *Elaeocarpus ganitrus* leaf research data and GC-MS profiling. To accentuate, the binding role of *Elaeocarpus ganitrus* phytochemicals with STAT3 receptor, their ADME properties and pharmacokinetic studies were investigated.

Materials and methods

Cell lines, chemicals and reagents

The chemicals and solvents used in the extraction and phytochemical analysis were of analytical grade, sourced from Sigma-Aldrich. MTT (3-[4,5-dimethylthiazol-2-yl]-2,5 diphenyl tetrazolium bromide) was also procured from Sigma-Aldrich. HeLa cells were obtained from the National Centre for Cell Sciences (NCCS), Pune, India. Fetal bovine serum and Dulbecco's Modified Eagle's Media were acquired from Gibco-life technologies.

Procurement of plant material

Fresh leaves of *E. ganitrus* were purchased from Patanjali Herbal Garden Nursery in Panchayanpur, Uttarakhand, India. Authentication of the *Elaeocarpus ganitrus* was conducted by the Department of Botany, Jamia Hamdard, New Delhi, India, and the voucher specimen was deposited at the University.

Method to prepare extracts

Leaves of *E. ganitrus* were carefully washed, air-dried for ten days, and ground to a fine powder. A sample of 1,000 grams of powder was exhaustively extracted three times with 100% methanol (10 times weight/volume) at room temperature for 72 h using a soxhlet apparatus. The resulting crude methanol extract was fractionated successively with solvents in increasing polarity order: heptane, chloroform, ethyl acetate, methanol, and water. The residue was air-dried and utilized for the subsequent solvents. The fractions obtained from each solvent were filtered, dried under vacuum using a rotary evaporator, and stored at 40 °C until use^[21].

Qualitative phytochemical analysis

The presence or absence of phytochemicals such as terpenoids, steroids, saponins, flavonoids, glycosides, tannins, and phenols in the chloroform and methanol extracts of *E. ganitrus* leaves was determined following the standard methodology^[22].

Cellular studies on HeLa cancer cell line

The HeLa cell line was stored in Dulbecco's Modified Eagle's Medium which is rich in 10% Fetal Bovine Serum, 1% antibiotic solution, 25 mM sodium bicarbonate, and 10 mM HEPES in a 5% CO₂ humidified atmosphere at 37 °C in an air jacketed incubator. The stock culture was perpetuated in the exponentially growing phase by passaging as, monolayer culture with 0.02% EDTA. Dislodged cells suspended in complete medium were routinely reseeded.

Cytotoxicity assay/MTT assay

The cytotoxic effects of the various fractions of *E. ganitrus* leaf on the HeLa cancer cell line were evaluated using the MTT assay. Cells were seeded overnight, and exposed to different concentrations of the prepared fractions (ranging from 50 to 200 µg/ml), and incubated for 48 h. After treatment, cells were incubated with MTT solution and the formazan crystals were solubilized and the absorbance was read at 570 nm^[23].

In silico investigation of phytochemicals obtained from leaf extracts

Binding energies of phytochemicals retrieved from plant leave extract with STAT3 were calculated by using software InstaDock for molecular docking. Discovery Studio Visualizer, and PyMOL, were used to visualize the chemical interactions of ligands and proteins. SWISS-ADME tool and ProTox-II were used for pharmacokinetic profiling studies. The X-ray crystal structure of STAT3 (PDB ID: 6NJS) was downloaded from

Protein Data Bank (PDB). All co-crystallized hetero atoms and attached water molecules and co-crystallized ligands, were eliminated from the original coordinates. The Polar hydrogen atoms were inculcated, the residue structures having lower occupancy were removed, and the incomplete side chains were then substituted by using ADT. Three-dimensional structures of phytocompounds were sketched using Chem3D.

Drug-likeness properties prognosis

Determination of the analogous behavior to the drug of phytoligands with the help of cheminformatics was done using online tool SwissADME developed by the Molecular Modelling Group, Swiss Institute of Bioinformatics^[24]. The computation of pharmacokinetics and physicochemical molecular properties help medicinal chemists in their routine drug discovery processes. Significant basic molecular information can be excavated from the chemical structure. The methods were preferred over other methods because of the speed, but also for the ease of interpreting results by fingerprinting method to enable researchers move through translation to medicinal chemistry and in molecular designing^[25].

Molecular docking-based virtual screening

The rationale behind molecular docking is to steer medicinal chemists for translational research. The affinity of a molecule to the receptor changes with small structural changes in the molecule^[26]. For molecular docking, STAT3 core complex PDB id (PMID: 31715132) was remodeled to ascertain binding energies with the best conformational poses of *Elaeocarpus ganitrus* leaves phytoligands. The InstaDock software is used to dock phytoligands with blind search space having a grid size of 110, 70, and 108 Å for X, Y, Z coordinates, correspondingly. The center of the grid was confined to X: 63.09, Y: 14.98, and Z: -76.91 axis, which covers all the heavy atoms embedded in the protein. The conformational site selected was so that the movement of the ligands was free to probe their best binding coordinates. Default docking specifications were employed to calculate various parameters. All the docking conformational poses were generated using PyMOL, a molecular visualization system and Discovery Studio Predictor.

Pharmacokinetic and toxicity prediction

Physicochemical parameters, water solubility, lipophilicity, pharmacokinetics, and drug-likeness were elicited from Swiss-ADME. To retrieve the toxicological profile of the phytoligands ProTox-II servers were employed^[27]. Early estimation of the Absorption, Distribution, Metabolism, Excretion and Toxicity abbreviated as ADMET imperative to ascribe the pharmacodynamics success of the lead phytoligands. (SMILES) strings to encode chemical structures were imported from PubChem, open chemistry database and implemented in SWISS-ADME tool^[24] to auspicate lipophilicity to show hydrophobic and hydrophilic nature, water solubility, necessary for absorption across membranes, and drug-likeness rules to assess metabolic profiles. Toxicology prediction of phytoligands is a crucial and fundamental aspect in the drug discovery process. ProTox-II is used to estimate computational toxicity, to accelerate the course to drug discovery, compute animal toxicity, and also help to attenuate animal experiments. In the PROTOX-II web server, toxicity classes are designated into four segments. Category I comprised of chemical entities with LD50 (LD = lethal Dose) values (LD50 ≤ 5) mg/kg, Category II comprised of compounds with LD50 values (5 < LD50 ≤ 50) mg/kg, Category III comprised of chemical entities having LD50 values

($50 < LD_{50} \leq 300$) mg/kg, Category IV comprised of compounds which have LD_{50} values ($300 < LD_{50} \leq 2,000$) mg/kg, Category V comprised of compounds with LD_{50} values ($2,000 < LD_{50} \leq 5,000$) mg/kg and Category VI comprised of compounds showing LD_{50} values ($LD_{50} > 5,000$) mg/kg^[28]. Category I and II manifested high toxicity, Category III and IV are comparatively less toxic and Category V and VI are considered to be non-toxic.

Results and discussion

The solvent extraction technique is usually employed to prepare extracts from plant materials attributable to its convenience to operate. The importance lies in that a large amount of plant material can be extracted with minimal solvent^[26]. Fresh leaves of *Elaeocarpus ganitrus* were purchased from Patanjali Herbal Garden Site Nursery located in Panchayanpur, Uttarakhand 249405, India. The confirmation of the authenticity of the *Elaeocarpus ganitrus* was done by the Department of Botany, Jamia Hamdard, New Delhi, India, and the leaf specimens deposited in the University. The crude methanol extract was unintermittently fractionated in the solvents heptane, chloroform, ethyl acetate, methanol, and water according to their increasing polarity^[16]. The anticancer activity of extracts was analyzed on the basis of their IC_{50} values. Cancerous HeLa cell line when treated with *E. ganitrus* leaf extracts exhibited a substantial inhibition of cells. The half maximal inhibitory concentration of chloroform and methanol extracts of *E. ganitrus* was ($IC_{50} = 304.39 \mu\text{g/ml}$) and ($IC_{50} = 308.59 \mu\text{g/ml}$) respectively followed by water ($IC_{50} = 340.14 \mu\text{g/ml}$), ethyl

acetate ($IC_{50} = 350.72 \mu\text{g/ml}$) and heptane ($IC_{50} = 381.76 \mu\text{g/ml}$) extracts (Fig. 1a–e & Fig. 2). The qualitative investigation using standard methodology^[22] of chloroform and methanol fractions of *E. ganitrus* leaves disinterred the presence of major phytochemicals namely steroids, saponins, terpenoids, tannins, phenols, glycosides and flavonoids Table 1. GC-MS analysis of the chloroform and methanolic fractions was done based on their lowest half maximal inhibitory concentration to get a complete profiling of the plant compounds. The peaks in the total ion current (TIC) chromatogram of GC-MS profile of the phytoligands commensurate with the spectrum of known chemical databases stockpiled in the GC-MS library. The gas chromatogram depicts the relative concentrations of different phytoligands getting eluted according to the retention time. The heights of the peak represent the comparative concentrations of the compounds present in the plant appear as peaks at different m/z ratios. The components present with their retention time, molecular formula, molecular weight and concentration (peak area %) are provided in Tables 2 & 3 showing the presence of 56 and 50 bioactive phytochemicals in the chloroform and methanol extracts respectively. Of 106 phytoligands obtained from chloroform and methanol extracts of *E. ganitrus* leaves, 81 phytoligands were identified as having the best drug-like properties following Lipinski's rule of five. Lipinski's rule states that molecular properties, physical or chemical of a compound are significant for a drug's pharmacokinetics behavior inside a biological system. The drug molecules that go along with the RO5 have fewer attrition rates when undergoing clinical trials. The cheminformatics study to identify

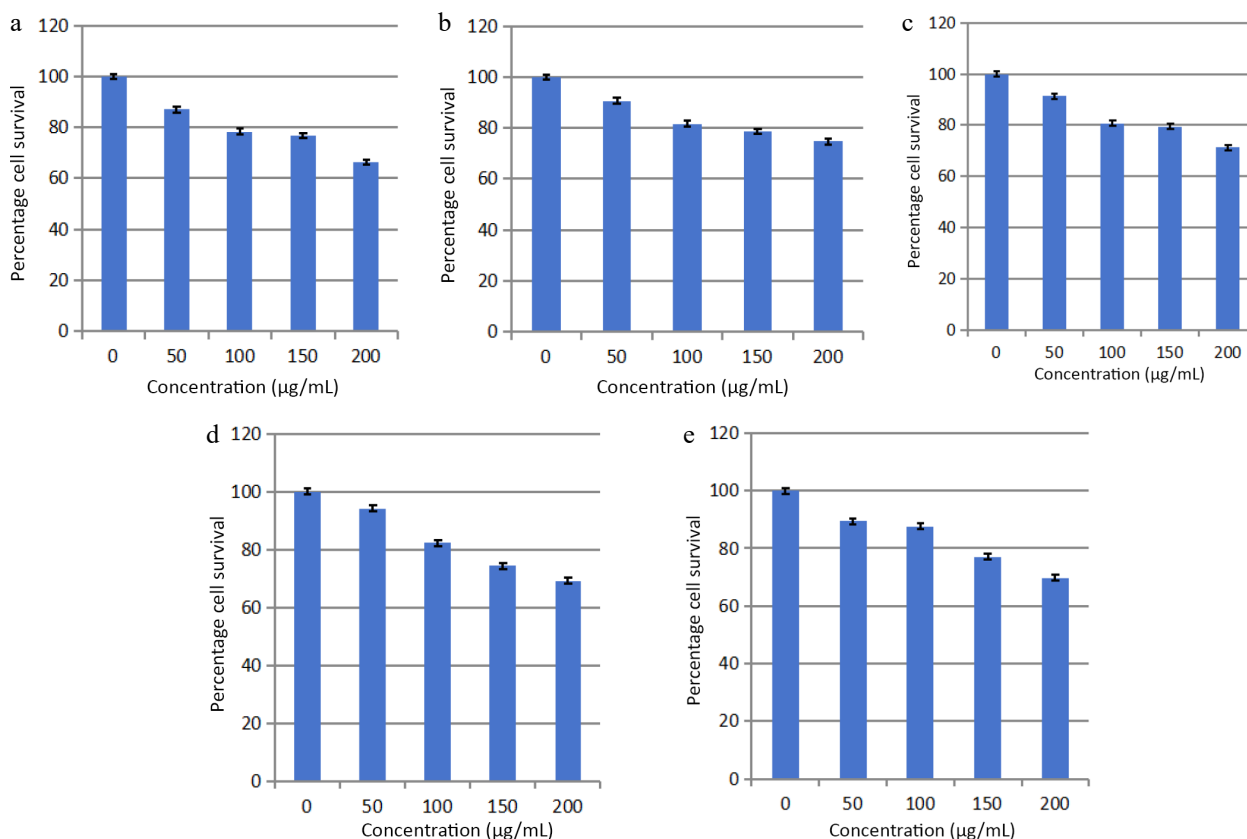


Fig. 1 Effects of (a) heptane, (b) chloroform, (c) methanol, (d) ethyl acetate and (e) water fractions of *E. ganitrus* leaves on the human cancer cell lines HeLa using MTT assay.

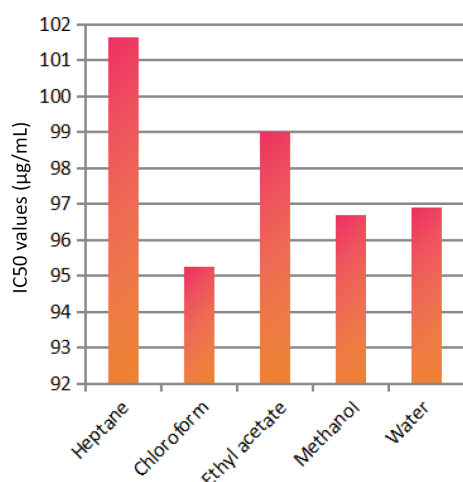


Fig. 2 IC₅₀ values of different extracts of *E. ganitrus* leaves against human cancer cell lines HeLa.

potential chemical entities having propensity for predefined biological targets is called virtual screening^[28]. To endeavor *in vitro* experiments time diminution, molecular docking-based virtual screening of 81 selected compounds with two reference inhibitors having substantial binding energies with 6NJS were preferred for further analysis. The STAT3 has dual nature as an oncogene or as a tumor suppressor during cancer progression. It has a SH₂ domain, linker domain, DNA binding domain, and all-alpha domain. The total energy of binding, Vander Waals forces, hydrogen bonding, electrostatic attraction, desolvation, and also a number of rotatable bonds present in the phytoligand, contribute to observe the free energy of binding of phytoligands with the receptor. Twenty-six (EG-1 to EG-26) compounds were selected as having appreciable binding affinities towards the 6NJS receptor (Table 4).

The absorption of drugs by the body is related to their pharmacokinetic properties and also cellular toxicity. The potency of the drug depends mostly on the pharmacokinetic parameters because ADME processes command the rate and extent of absorption when an administered dose of a drug approaches to its action site. Hence, *in silico* pharmacokinetic profile of filtered compounds was surveyed to gather the putative bioavailability data for receptor 6NJS. The cumulative findings for pharmacokinetics profiling, bioavailability data, drug-likeness properties and drug friendliness and toxicity effects of selected 26 phytoligands with known inhibitors (Plumbagin and Sanguinarine) are given in Tables 5–10. The prediction revealed that the six molecules (EG-9, EG-12, EG-13, EG-16, and EG-26) can be lead compounds for new drug candidates for anti-cancer phytomedicine. The Half maximal Inhibitory concentration of EG-13 was (IC₅₀ = 254.29 µg/ml) further support our results (Fig. 3).

In Table 5, for pharmacokinetics prognostication, the gastrointestinal (GI) absorption rate was fetched for all preferred six phytoligands and both reference drugs. The blood-brain permeability was seen as positive for all the six phytoligands and both reference drugs. The prediction of bioavailability (Table 6) demonstrated that similar bioavailability scores were observed for all the filtered six phytoligands (0.55) like reference drugs. The water solubility data showed all the six compounds and plumbagin are soluble while Sanguinarine is poorly soluble. For drug-likeness prediction (Table 7), all the six compounds and both known inhibitors

Table 1. Qualitative analysis of phytochemicals in *E. ganitrus* leaf extracts.

Tested compounds	Chloroform extract	Methanol extract
Steroids	+	+
Terpenoids	+	+
Saponins	+	+
Glycosides	+	+
Tannins	+	+
Flavonoids	+	+
Phenols	+	+

+ → Present; – → Absent.

were obtained suitable for the Lipinski rule as zero violation. For Ghose, Veber, and Egan filter 0 violation was obtained for all the six phytoligands and both inhibitors. In the case of medicinal chemistry friendliness prediction (Table 8), the PAINS structural alert obtained 0 violations for all the six phytoligands and sanguinarine while two alerts for plumbagin. Table 9 shows EG-9 belongs to the non-toxic class VI, EG-15, and EG-16 also belong to the non-toxic class V, EG-12, EG-13, EG-26 and Sanguinarine belongs to the less toxic class IV while plumbagin belongs to the high-toxic class II. The bioavailability radar (Fig. 3) for phytoligands depicting bioavailability prognostic showed that all six phytoligands were found within the data range of lipophilicity nature ($-0.7 < \text{XLOGP3} < +5.0$), molecule size ($150 \text{ g/mol} < \text{MW} < 500 \text{ g/mol}$), polarity ($20 \text{ \AA}^2 < \text{TPSA} < 130 \text{ \AA}^2$), insolubility [$-6 < \text{LogS (ESOL)} < 0$], insaturation ($0.25 < \text{Fraction Csp3} < 1$) and flexible bonds ($0 < \text{Num. rotatable bonds} < 9$) and colored part of radar while known inhibitors plumbagin and sanguinarine does not fit the bioavailability radar (Table 10). As mentioned in Table 5, all the phytoligands and reference compounds have higher gastrointestinal (GI) absorption rates, therefore they can instantly be absorbed by the human intestine. All phytoligands have the ability to pass the blood brain barrier (BBB permeant) and values for the aqueous solubility (log S) of the phytochemicals fall in the recommended range that is -1 to -5 ^[29], thus, have improved absorption and distribution properties. The bioavailability scores were identical for all six molecules, standing at 0.55, similar to the reference drugs. In drug-likeness prediction, none of the six compounds and both known inhibitors violated the Lipinski rule, Ghose, Veber, and Egan filters. Regarding medicinal chemistry friendliness, the PAINS structural alert identified zero violations for all six phytoligands and Sanguinarine, whereas Plumbagin had two alerts. Table 9 revealed that EG-9 belonged to the non-toxic class VI, while EG-15 and EG-16 were in harmless class V. Other compounds EG-12, EG-13, EG-26 and sanguinarine was from less harmful class IV which could be modified to a non-toxic class during the lead optimization stage of drug discovery^[30] while selected standard plumbagin showed high toxic class II. Drug-induced hepatotoxicity often lead to abrupt liver failure and drug rejections^[31]. Drug-induced liver injury might be long-term or occur only once. Obviously, the selected compounds and standards are non-hepatotoxic. The bioavailability radar (Fig. 4) depicted that all six phytoligands were within the data range for oral bioavailability prediction. Conversely, standards plumbagin and sanguinarine did not fit within the bioavailability radar. The pink area shown in the radar corresponds to the most promising zone for all the bioavailability properties. In Table 10, all the phytochemicals satisfied 150 g/mol and 500 g/mol criteria for (SIZE) of good drug candidates. The polarity (POLAR) was observed with the Total Polarity Surface Area (TPSA) and all the phytochemicals

Table 2. GC–MS analysis of chloroform fraction of *E. ganitrus* leaves.

Peak no.	R. Time	Area	Area %	Name
1	7.328	3392451	3.60	Phenol, 2-methoxy-4-(2-propenyl)-
2	7.494	432542	0.46	Cyclododecane
3	7.925	5018874	5.32	Bicyclo[7.2.0]undec-4-ene,4,11,11-trimethyl-8-methylene-
4	8.392	264573	0.28	1,4,8-Cycloundecatriene, 2,6,6,9-tetramethyl-,(e,e,e)-
5	9.137	1568546	1.66	Phenol, 3,5-bis(1,1-dimethylethyl)-
6	10.016	2727130	2.89	1-Heptadecene
7	12.221	2959933	3.14	1-Octadecene
8	12.670	178963	0.19	Neophytadiene
9	12.782	147893	0.16	2-Pentadecanone, 6,10,14-trimethyl-
10	13.496	127511	0.14	7,9-Di-tert-butyl-1-oxaspiro(4,5)deca-6,9-diene-2,8-dione
11	13.594	2105374	2.23	Hexadecanoic acid, methyl ester
12	13.801	186096	0.20	Isophytol
13	14.003	2582987	2.74	Dibutyl phthalate
14	14.233	126402	0.14	1-Nonadecene
15	15.143	262912	0.28	1-Octadecanol
16	15.196	409325	0.43	9,12-Octadecadienoic acid (z,z)-, methyl ester
17	15.256	1418833	1.50	9,12,15-Octadecatrienoic acid, methyl ester, (z,z,z)-
18	15.396	8267193	8.76	P-menth-1-ene-3,3-d2
19	15.776	4268486	4.53	Cholest-24-ene, (5.alpha.,20.xi.)-
20	16.081	1835125	1.95	Behenic alcohol
21	17.015	574682	0.61	Glycidyl palmitate
22	17.502	356762	0.38	4,8,12,16-Tetramethylheptadecan-4-olide
23	17.792	1548266	1.64	N-tetracosanol-1
24	18.507	892966	0.95	Glycidyl oleate
25	18.633	387075	0.41	Pentacosane
26	18.885	1160812	1.23	Hexadecanoic acid, 2-hydroxy-1-(hydroxymethyl)ethyl ester
27	18.949	2520126	2.67	1,2-Benzenedicarboxylic acid
28	19.383	1722880	1.83	Hexacosyl pentafluoropropionate
29	19.997	295789	0.31	Carbonic acid, propyl 3,5-difluorophenyl ester
30	20.152	1655981	1.76	Tetracontane
31	20.287	718350	0.76	9-Octadecenoic acid (z)-, 2,3-dihydroxypropyl ester
32	20.437	1633424	1.73	Octadecanoic acid, 2,3-dihydroxypropyl ester
33	20.875	8530902	9.04	Carbonic acid, eicosyl prop-1-en-2-yl ester
34	21.225	1169791	1.24	.alpha.-tocospiro b
35	21.371	1475710	1.56	.alpha.-tocospiro b
36	21.566	2790793	2.96	Tetracosane
37	21.619	566554	0.60	1-Heptacosanol
38	21.978	208285	0.22	Tetracontane
39	22.244	3146831	3.34	Tetracontane
40	22.339	198857	0.21	Triacetyl acetate
41	22.758	602558	0.64	.gamma.-tocopherol
42	22.987	3769661	4.00	Tetracontane
43	23.083	307563	0.33	Octacosanol
44	23.368	804368	0.85	2,5,7,8-Tetramethyl-2-(4,8,12-trimethyltridecyl)-3,4-dihydro-2h-chromen-6-yl hexofuranoside
45	23.832	2825781	3.00	Hexatriacontane
46	24.442	224749	0.24	Ergost-5-en-3-ol
47	24.697	146326	0.16	2,6,10,15,19,23-Hexamethyl-tetracos-2,10,14,18,22-pentaene-6,7-diol
48	24.816	2579206	2.73	Tetracontane
49	25.344	4403683	4.67	.gamma.-sitosterol
50	25.897	247451	0.26	Phenol, 2,4-bis(1,1-dimethylethyl)-, phosphite (3:1)
51	25.971	1050990	1.11	Tetracontane
52	27.369	1062263	1.13	Tetracontane
53	29.049	4468338	4.74	Benzenepropanoic acid, 3,5-bis(1,1-dimethylethyl)-4-hydroxy-,octadecyl ester
54	31.061	859726	0.91	Tetrapentacontane
55	33.505	689017	0.73	Tetrapentacontane
56	36.515	570264	0.60	Tetrapentacontane

Table 3. GC–MS analysis of methanol fraction of *E. ganitrus* leaves.

Peak no.	R. time	Area	Area %	Name
1	4.562	1716062	2.75	4h-pyran-4-one, 2,3-dihydro-3,5-dihydroxy-6-methyl-
2	5.545	132891	0.21	1,5-Dimethyl-1-vinyl-4-hexenyl 2-aminobenzoate
3	6.130	66420	0.11	E-6-octadecen-1-ol acetate
4	6.658	9826941	15.75	4-Hydroxy-3-methylacetophenone
5	7.421	59260	0.09	1-Undecanol
6	7.746	290020	0.46	Methyl2,3,6,7-tetra-o-acetyl-4-o-methyl-.beta.-glycero-d-glucoheptopyranoside
7	8.935	1932769	3.10	Guanosine
8	9.178	535822	0.86	1,3:2,5-Dimethylene-l-ramnitol
9	9.949	463870	0.74	Octadecanoic acid
10	10.144	279041	0.45	1,2-Benzenedicarboxylic acid, diethyl este
11	10.370	1683966	2.70	.alpha.-methyl-l-sorboiside
12	10.606	1300727	2.08	.alpha.-d-galactopyranoside, methyl
13	10.920	280573	0.45	Butanoic acid, 3-methyl-, hexahydro-4- methylspiro[cyclopenta[c]pyran-7(1h),2'-oxirane]-1,6-diyl ester
14	11.090	80380	0.13	Tricyclo[7.2.0.0(2,6)]undecan-5-ol, 2,6,10,10-tetramethyl- (isomer 3)
15	11.224	161606	0.26	.alpha.-d-galactopyranoside, methyl
16	11.492	189485	0.30	Octadecanoic acid, methyl ester
17	12.437	260634	0.42	2(4h)-benzofuranone, 5,6,7,7a-tetrahydro-6- hydroxy-4,4,7a-trimethyl-, (6s-cis)-
18	12.643	123768	0.20	Neophytadiene
19	13.565	2866045	4.59	Hexadecanoic acid, methyl ester
20	13.780	34044	0.05	1-hexadecen-3-ol, 3,5,11,15-tetramethyl-
21	13.910	47535	0.08	Silane, ethenylethylidimethyl-
22	14.555	73535	0.12	Pentadecanoic acid, methyl ester
23	15.188	1768899	2.83	9,12-Octadecadienoic acid (z,z)-, methyl ester
24	15.249	5971407	9.57	(9e,12e)-9,12-octadecadienoyl chloride #
25	15.385	7933212	12.71	1,1'-Bicyclohexyl, 2-methyl-, cis-
26	15.481	910073	1.46	Methyl stearate
27	15.758	8239629	13.21	Cholest-24-ene, (5.alpha.,20.xi.)-
28	16.075	396431	0.64	Methyl octadeca-9,12-dienoate
29	16.444	77246	0.12	Methyl 4-(dimethylamino)bicyclo[2.2.2]oct- 5-ene-2-carboxylate
30	16.612	54809	0.09	Hexadecanoic acid, 2-hydroxy-1-(hydroxymethyl)ethyl ester
31	16.999	215619	0.35	17-octadecynoic acid
32	17.249	219061	0.35	Eicosanoic acid, methyl ester
33	18.127	232480	0.37	Oleoyle chloride
34	18.509	301125	0.48	Undec-10-ynoic acid, undec-2-en-1-yl ester
35	18.705	135332	0.22	Hexadecanoic acid, 1-(hydroxymethyl)-1,2-ethanediyl ester
36	18.899	4607864	7.38	Hexadecanoic acid, 2-hydroxy-1-(hydroxymethyl)ethyl ester
37	19.655	106312	0.17	Hexadecanoic acid, methyl ester
38	20.300	580671	0.93	Oleoyle chloride
39	20.462	994304	1.59	Octadecanoic acid, 2,3-dihydroxypropyl ester
40	20.912	3584027	5.74	9-octadecenamide
41	21.225	221450	0.35	.alpha.-tocospiro b
42	21.378	384165	0.62	.alpha.-tocospiro b
43	21.626	175973	0.28	Eicosyl heptafluorobutyrate
44	21.803	89987	0.14	Hexacosanoic acid, methyl ester
45	22.769	160960	0.26	.gamma.-tocopherol
46	22.989	86757	0.14	Tetracontane
47	23.174	92442	0.15	Stigmast-5-en-3-ol, (3.beta.)-
48	23.380	1030143	1.65	Vitamin e
49	25.372	1237263	1.98	.gamma.-sitosterol
50	27.084	183826	0.29	Di-o-acetyltetrahydrostapelogenin

show good TPSA values. Besides, the flexibility (FLEX) property evaluated by the number of rotatable bonds falls within the recommended range. Lipophilicity (LIPO) and insolubility (INSOLU) were evaluated and come in the range The Unsaturation (INSATU) was calculated using Fraction Csp3 falls within a

recommended range of $0.25 < \text{Fraction Csp3} < 1$) for all phytoligands. However, Plumbagin and Sanguinarine exhibit lower values (0.09 and 0.15, respectively).

2D and 3D interactions of the five phytoligands (EG-9, EG-12, EG-13, EG-15, EG-16 and EG-26) with 6njs are shown in Table 11.

Table 4. Docking results of 81 phytoligands.

S. no.	Name of the ligand	Binding free energy (kcal/mol)	pKi	Ligand efficiency (kcal/mo/non-H atom)	Torsional energy
1	Phenol, 2-methoxy-4-(2-propenyl)-	-5.6	4.11	0.4667	1.2452
2	Cyclododecane	-5.9	4.33	0.4917	0
3	Bicyclo[7.2.0]undec-4-ene,4,11,11-trimethyl-8-methylene-	-6.6	4.84	0.44	0
4	1,4,8-Cycloundecatriene, 2,6,6,9-tetramethyl-,(e,e,e)-	-6.5	4.77	0.4333	0
5	Phenol, 3,5-bis(1,1-dimethylethyl)-	-6.5	4.77	0.4333	0.9339
6	1-Heptadecene	-4.6	3.37	0.2706	4.3582
7	1-Octadecene	-4	2.93	0.2	4.0469
8	Neophytadiene	-5.9	4.33	0.295	4.0469
9	2-Pentadecanone, 6,10,14-trimethyl-	-5.4	3.96	0.2842	3.7356
10	7,9-Di-tert-butyl-1-oxaspiro(4,5)deca-6,9-diene-2,8-dione	-6.5	4.77	0.325	0.6226
11	Hexadecanoic acid, methyl ester	-4.9	3.59	0.2579	4.6695
12	Isophytol	-4.9	3.59	0.2333	4.3582
13	Dibutyl phthalate	-5.2	3.81	0.26	3.113
14	1-Nonadecene	-4.9	3.59	0.2579	4.9808
15	1-octadecanol	-5	3.67	0.2632	5.2921
16	9,12-Octadecadienoic acid (z,z)-, methyl ester	-5	3.67	0.2381	4.6695
17	9,12,15-Octadecatrienoic acid, methyl ester, (z,z,z)-	-5.4	3.96	0.2571	4.3582
18	P-Menth-1-ene-3,3-d2	-4.9	3.59	0.49	0.3113
19	Behenic alcohol	-4.7	3.45	0.2043	6.5373
20	Glycidyl palmitate	-5.4	3.96	0.2842	3.7356
21	4,8,12,16-Tetramethylheptadecan-4-olide	-6.3	4.62	0.2739	3.7356
22	N-tetracosanol-1	-4.4	3.23	0.176	7.1599
23	Glycidyl oleate	-4.6	3.37	0.1917	5.6034
24	Pentacosane	-4.7	3.45	0.188	6.8486
25	Hexadecanoic acid, 2-hydroxy-1-(hydroxymethyl)ethyl ester	-4.6	3.37	0.2	6.226
26	1,2-Benzenedicarboxylic acid	-5.7	4.18	0.475	1.2452
27	Carbonic acid, propyl 3,5-difluorophenyl ester	-6.1	4.47	0.4067	1.5565
28	9-Octadecenoic acid (z)-, 2,3-dihydroxypropyl ester	-5	3.67	0.2	6.5373
29	Octadecanoic acid, 2,3-dihydroxypropyl ester	-4.9	3.59	0.196	6.8486
30	Carbonic acid, eicosyl prop-1-en-2-yl ester	-5.1	3.74	0.1889	6.8486
31	Tetracosane	-4.9	3.59	0.2042	6.5373
32	1-Heptacosanol	-5.1	3.74	0.1821	8.0938
33	Triacetyl acetate	-3.9	2.86	0.1147	9.339
34	Gamma.-tocopherol	-6.8	4.99	0.2267	4.0469
35	Octacosanol	-4.2	3.08	0.1448	8.4051
36	2,5,7,8-Tetramethyl-2-(4,8,12-trimethyltridecyl)-3,4-dihydro-2h-chromen-6-yl hexofuranoside	-7.2	5.28	0.1714	6.226
37	Ergost-5-en-3-ol	-7.3	5.35	0.2517	1.8678
38	2,6,10,15,19,23-Hexamethyl-tetracos-2,10,14,18,22-pentaene-6,7-diol	-6	4.4	0.1875	5.6034
39	Gamma.-sitosterol	-9	6.6	0.3	2.1791
40	4h-pyran-4-one,2,3-dihydro-3,5-dihydroxy-6-methyl-	-5	3.67	0.5	0.6226
41	1,5-Dimethyl-1-vinyl-4-hexenyl 2-aminobenzoate	-6.4	4.69	0.32	2.4904
42	E-6-octadecen-1-ol acetate	-4.7	3.45	0.2136	5.2921
43	4-Hydroxy-3-methylacetophenone	-5.7	4.18	0.5182	0.6226
44	1-undecanol	-4.5	3.3	0.375	3.113
45	Methyl2,3,6,7-tetra-o-acetyl-4-o-methyl-.beta.-glycero-d-glucoheptopyranoside	-5.5	4.03	0.1964	3.7356
46	Guanosine	-6.8	4.99	0.2615	1.5565
47	1,3:2,5-Dimethylene-l-rhamnitol	-5.4	3.96	0.4154	0.3113
48	Octadecanoic acid	-5.3	3.89	0.265	5.2921
49	1,2-benzenedicarboxylic acid, diethyl este	-5.4	3.96	0.3375	1.8678
50	.alpha.-methyl-l-sorbose	-4.7	3.45	0.3615	1.8678
51	.alpha.-d-galactopyranoside, methyl	-5.2	3.81	0.4	1.8678
52	Butanoic acid, 3-methyl-, hexahydro-4- methylspiro[cyclopenta[c]pyran-7(1h),2'-oxirane]-1,6-diyl ester	-6.8	4.99	0.2267	3.4243
53	Tricyclo[7.2.0.0(2,6)]undecan-5-ol, 2,6,10,10-tetramethyl- (isomer 3)	-6.5	4.77	0.4062	0.3113
54	.alpha.-d-galactopyranoside, methyl	-5.3	3.89	0.4077	1.8678
55	Octadecanoic acid, methyl ester	-4.1	3.01	0.1952	5.2921
56	2(4h)-benzofuranone, 5,6,7,7a-tetrahydro-6- hydroxy-4,4,7a-trimethyl-, (6s-cis)-	-6.5	4.77	0.4643	0.3113
57	Neophytadiene	-5	3.67	0.25	4.0469
58	Hexadecanoic acid, methyl ester	-4.9	3.59	0.2579	4.6695
59	1-Hexadecen-3-ol, 3,5,11,15-tetramethyl-	-5.7	4.18	0.2714	4.3582
60	Pentadecanoic acid, methyl ester	-4.4	3.23	0.2444	4.3582

(to be continued)

Table 4. (continued)

S. no.	Name of the ligand	Binding free energy (kcal/mol)	pKi	Ligand efficiency (kcal/mo/non-H atom)	Torsional energy
61	9,12-Octadecadienoic acid (z,z)-, methyl ester	-5.4	3.96	0.2571	4.6695
62	(9e,12e)-9,12-octadecadienoyl chloride #	-4.7	3.45	0.235	4.3582
63	1,1'-bicyclohexyl, 2-methyl-, cis-	-5.6	4.11	0.4308	0.3113
64	Methyl stearate	-5	3.67	0.2381	5.2921
65	Cholest-24-ene, (5.alpha.,20.xi.)-	-9.2	6.75	0.3407	1.2452
66	Methyl octadeca-9,12-dienoate	-4.5	3.3	0.2143	4.6695
67	Methyl 4-(dimethylamino)bicyclo[2.2.2]oct- 5-ene-2-carboxylate	-5.7	4.18	0.38	0.9339
68	Hexadecanoic acid, 2-hydroxy-1-(hydroxymethyl)ethyl ester	-4.8	3.52	0.2087	6.226
69	17-octadecynoic acid	-5.1	3.74	0.255	5.2921
70	Eicosanoic acid, methyl ester	-4.8	3.52	0.2087	5.9147
71	Undec-10-ynoic acid, undec-2-en-1-yl ester	-5.1	3.74	0.2125	5.9147
72	Hexadecanoic acid, 2-hydroxy-1-(hydroxymethyl)ethyl ester	-4.7	3.45	0.2043	6.226
73	Hexadecanoic acid, methyl ester	-4.5	3.3	0.2368	4.6695
74	Oleoyl chloride	-4.6	3.37	0.23	4.6695
75	Octadecanoic acid, 2,3-dihydroxypropyl ester	-4.6	3.37	0.184	6.8486
76	9-octadecenamide	-4.7	3.45	0.235	4.6695
77	.alpha.-tocospiro b	-6.4	4.69	0.1939	4.3582
78	Eicosyl heptafluorobutyrate	-5.6	4.11	0.1697	7.1599
79	Hexacosanoic acid, methyl ester	-4.7	3.45	0.1621	7.7825
80	Stigmast-5-en-3-ol, (3.beta.)-	-7.6	5.57	0.2533	2.1791
81	Vitamin e	-7.1	5.21	0.229	4.0469
82	Plumbagin	-5.9	4.33	0.4214	0.3113
83	Sanguinarine	-8.9	6.53	0.356	0

Table 5. Pharmacokinetics prediction of phytoligands established in *E. ganitrus*.

S. no.	Phytochemical	Gastro-intestinal absorption	Blood-brain permeant	P-glycoprotein substrate	CYP450 1A2 inhibitor	CYP450 2C19 inhibitor	CYP450 2C9 inhibitor	CYP450 2D6 inhibitor	CYP450 3A4 inhibitor	Skin permeation as log Kp (cm/s)
EG-1	Cholest-24-ene, (5.alpha.,20.xi.)-	Low	No	No	No	No	Yes	No	No	-1.02
EG-2	gamma.-sitosterol	Low	No	No	No	No	No	No	No	-2.65
EG-3	Stigmast-5-en-3-ol, (3.beta.)-	Low	No	No	No	No	No	No	No	-2.20
EG-4	Ergost-5-en-3-ol	Low	No	No	No	No	No	No	No	-2.50
EG-5	2,5,7,8-Tetramethyl-2-(4,8,12-trimethyltridecyl)-3,4-dihydro-2h-chromen-6-yl hexofuranoside	Low	No	No	No	No	No	No	Yes	-3.60
EG-6	Vitamin e	Low	No	Yes	No	No	No	No	No	-1.33
EG-7	Guanosine	Low	No	No	No	No	No	No	No	-9.37
EG-8	gamma.-tocopherol	Low	No	Yes	No	No	No	No	No	-1.51
EG-9	Butanoic acid, 3-methyl-, hexahydro-4-methylspiro[cyclopenta[c]pyran-7(1h),2'-oxirane]-1,6-diyl ester	High	Yes	No	No	No	No	Yes	Yes	-6.18
EG-10	Bicyclo[7.2.0]undec-4-ene,4,11,11-trimethyl-8-methylene-	Low	No	No	No	Yes	Yes	No	No	-4.44
EG-11	1,4,8-Cycloundecatriene, 2,6,6,9-tetramethyl-,(e,e,e)-	Low	No	No	No	No	Yes	No	No	-4.32
EG-12	Phenol, 3,5-bis(1,1-dimethylethyl)-	High	Yes	No	No	No	No	Yes	No	-4.07
EG-13	7,9-Di-tert-butyl-1-oxaspiro(4,5)deca-6,9-diene-2,8-dione	High	Yes	No	No	Yes	Yes	No	No	-5.28
EG-14	2(4h)-benzofuranone, 5,6,7,7a-tetrahydro-6- hydroxy-4,4,7a-trimethyl-, (6s-cis)-	High	Yes	No	No	No	No	No	No	-6.79
EG-15	Tricyclo[7.2.0.0(2,6)]undecan-5-ol, 2,6,10,10-tetramethyl-(isomer 3)	High	Yes	No	No	Yes	Yes	No	No	-4.75
EG-16	1,5-Dimethyl-1-vinyl-4-hexenyl 2-aminobenzoate	High	Yes	No	No	Yes	Yes	No	No	-4.54
EG-17	alpha.-tocospiro b	High	No	No	No	No	No	No	No	-3.90
EG-18	4,8,12,16-Tetramethylheptadecan-4-olide	Low	No	No	Yes	No	Yes	No	No	-2.70
EG-19	Carbonic acid, propyl 3,5-difluorophenyl ester	High	Yes	No	Yes	Yes	No	No	No	-5.37
EG-20	2,6,10,15,19,23-Hexamethyl-tetracos-2,10,14,18,22-pentaene-6,7-diol	Low	No	No	Yes	No	Yes	No	No	-2.37
EG-21	Cyclododecane	Low	No	No	No	No	No	No	No	-4.42
EG-22	Neophytadiene	Low	No	Yes	No	No	Yes	No	No	-1.17
EG-23	1,2-Benzenedicarboxylic acid	High	No	No	No	No	No	No	No	-6.80
EG-24	4-Hydroxy-3-methylacetophenone	High	Yes	No	Yes	No	No	No	No	-6.54
EG-25	1-Hexadecen-3-ol, 3,5,11,15-tetramethyl-	Low	No	Yes	No	No	Yes	No	No	-2.41
EG-26	Methyl 4-(dimethylamino)bicyclo[2.2.2]oct- 5-ene-2-carboxylate	High	Yes	No	No	No	No	No	No	-6.65
	Plumbagin	High	Yes	No	Yes	No	No	No	No	-5.82
	Sanguinarine	High	Yes	Yes	Yes	Yes	No	No	No	-5.17

Table 6. Bioavailability prediction of phytoligands established in *E. ganitrus*.

Phyto-ligands	Bioavailability score	Water solubility as logS	iLOGP	XLOGP3	WLOGP	MLOGP	SILICOS-IT
EG-1	0.55	Poorly soluble as -6.25	5.12	10.62	8.42	8.32	7.14
EG-2	0.55	Poorly soluble as -6.19	4.75	8.86	7.96	5.80	7.04
EG-3	0.55	Poorly soluble as -6.19	4.79	9.34	8.02	6.73	7.04
EG-4	0.55	Moderately soluble as -5.79	4.92	8.80	7.63	6.54	6.63
EG-5	0.55	Poorly soluble as -7.37	6.14	8.89	6.31	3.49	8.12
EG-6	0.55	Poorly soluble as -9.16	5.92	10.70	8.84	6.14	9.75
EG-7	0.55	Very Soluble as 0.51	-0.23	-1.89	-3.00	-2.76	-2.22
EG-8	0.55	Poorly soluble as -8.79	5.76	10.33	8.53	5.94	9.20
EG-9	0.55	Soluble as -2.86	3.87	3.34	2.93	2.07	3.34
EG-10	0.55	Soluble as -3.77	3.29	4.38	4.73	4.63	4.19
EG-11	0.55	Soluble as -3.52	3.27	4.55	5.04	4.53	3.91
EG-12	0.55	Soluble as -4.25	2.86	4.91	3.99	3.87	3.81
EG-13	0.55	Soluble as -3.81	2.91	3.81	3.59	2.87	3.82
EG-14	0.55	Very Soluble as -1.82	1.88	1.00	1.41	1.49	1.86
EG-15	0.55	Soluble as -3.18	3.01	4.09	3.61	3.81	3.40
EG-16	0.55	Moderately soluble as -4.28	3.37	4.83	4.12	3.63	3.75
EG-17	0.55	Poorly soluble as -7.19	4.94	7.24	6.58	3.67	7.85
EG-18	0.55	Poorly soluble as -6.31	4.15	7.86	6.52	4.96	6.99
EG-19	0.55	Soluble as -3.59	2.84	3.17	3.73	2.91	2.81
EG-20	0.55	Poorly soluble as -6.30	6.11	9.38	8.77	6.01	9.10
EG-21	0.55	Soluble as -3.21	3.01	4.10	4.68	5.00	4.00
EG-22	0.55	Poorly soluble as -6.11	5.05	9.62	7.17	6.21	7.30
EG-23	0.85	Soluble as -1.14	0.60	0.73	1.08	1.20	0.61
EG-24	0.55	Very Soluble as -2.53	1.54	0.95	1.90	1.44	2.14
EG-25	0.55	Moderately soluble as -5.51	4.97	8.02	6.36	5.25	6.57
EG-26	0.55	Very Soluble as -1.35	2.70	1.31	1.45	1.77	1.11
Plumbagin	0.55	Soluble as -2.85	1.79	2.29	1.72	0.59	2.22
Sanguinarine	0.55	Poorly soluble as -6.09	-0.04	4.45	3.43	2.72	3.85

Table 7. Drug-likeness prediction of phytoligands established in *E. ganitrus*.

Phyto-ligands	Lipinski rule	Ghose filter	Veber filter	Egan filter	Muegge filter
EG-1	Yes	No	Yes	No	No
EG-2	Yes	No	Yes	No	No
EG-3	Yes	No	Yes	No	No
EG-4	Yes	No	Yes	No	No
EG-5	Yes	No	No	No	No
EG-6	Yes	No	No	No	No
EG-7	Yes	No	No	No	No
EG-8	Yes	No	No	No	No
EG-9	Yes	Yes	Yes	Yes	Yes
EG-10	Yes	Yes	Yes	Yes	Yes
EG-11	Yes	Yes	Yes	Yes	Yes
EG-12	Yes	Yes	Yes	Yes	No
EG-13	Yes	Yes	Yes	Yes	Yes
EG-14	Yes	Yes	Yes	Yes	No
EG-15	Yes	Yes	Yes	Yes	No
EG-16	Yes	Yes	Yes	Yes	Yes
EG-17	Yes	No	No	No	No
EG-18	Yes	No	No	No	No
EG-19	Yes	Yes	Yes	Yes	Yes
EG-20	Yes	No	No	No	No
EG-21	Yes	Yes	Yes	Yes	No
EG-22	Yes	No	No	No	No
EG-23	Yes	No	Yes	Yes	No
EG-24	Yes	No	Yes	Yes	No
EG-25	Yes	No	No	No	No
EG-26	Yes	Yes	Yes	Yes	Yes
Plumbagin	Yes	Yes	Yes	Yes	No
Sanguinarine	Yes	Yes	Yes	Yes	Yes

Table 8. Medicinal chemistry prediction of phytoligands established in *E. ganitrus*.

Sl. No.	PAINS structural alert	Brenk structural alert	Lead-likeness	Synthetic accessibility score
EG-1	0	1	2	5.61
EG-2	0	1	2	6.42
EG-3	0	1	2	6.30
EG-4	0	1	2	6.17
EG-5	0	0	3	7.10
EG-6	0	0	3	5.17
EG-7	0	0	0	3.86
EG-8	0	0	3	5.00
EG-9	0	2	2	5.59
EG-10	0	1	2	4.51
EG-11	0	1	2	3.66
EG-12	0	0	2	1.37
EG-13	0	0	1	4.35
EG-14	0	0	1	3.63
EG-15	0	0	2	3.77
EG-16	0	2	1	2.91
EG-17	0	0	3	6.76
EG-18	0	0	2	4.12
EG-19	0	1	1	2.23
EG-20	0	1	3	5.52
EG-21	0	0	2	2.21
EG-22	0	1	2	4.08
EG-23	0	0	1	1.00
EG-24	0	0	1	1.00
EG-25	0	1	2	3.89
EG-26	0	1	1	4.38
Plumbagin	2	0	1	2.41
Sanguinarine	0	2	1	2.59

Table 9. Toxicity prediction of phytoligands established in *E. ganitrus*.

Phyto-ligands	LD ₅₀ (mg/kg)	Toxicity class	Hepatotoxicity	Carcinogenicity	Immunotoxicity	Mutagenicity	Cytotoxicity
EG-1	5000	5	Inactive	Inactive	Active	Inactive	Inactive
EG-2	890	4	Inactive	Inactive	Active	Inactive	Inactive
EG-3	890	4	Inactive	Inactive	Active	Inactive	Inactive
EG-4	890	4	Inactive	Inactive	Active	Inactive	Inactive
EG-5	3000	5	Inactive	Inactive	Active	Inactive	Inactive
EG-6	5000	5	Inactive	Inactive	Inactive	Inactive	Inactive
EG-7	13	2	Inactive	Inactive	Inactive	Inactive	Inactive
EG-8	5000	5	Inactive	Inactive	Inactive	Inactive	Inactive
EG-9	8000	6	Inactive	Active	Inactive	Active	Inactive
EG-10	5300	5	Inactive	Inactive	Active	Inactive	Inactive
EG-11	3650	5	Inactive	Inactive	Inactive	Inactive	Inactive
EG-12	800	4	Inactive	Inactive	Inactive	Inactive	Inactive
EG-13	900	4	Inactive	Inactive	Inactive	Inactive	Inactive
EG-14	34	2	Inactive	Active	Inactive	Inactive	Inactive
EG-15	2050	5	Inactive	Inactive	Inactive	Inactive	Inactive
EG-16	4250	5	Inactive	Inactive	Inactive	Inactive	Inactive
EG-17	300	3	Inactive	Inactive	Inactive	Inactive	Active
EG-18	4400	5	Inactive	Inactive	Inactive	Inactive	Inactive
EG-19	1500	4	Inactive	Inactive	Inactive	Inactive	Inactive
EG-20	4300	5	Inactive	Inactive	Inactive	Inactive	Inactive
EG-21	750	3	Inactive	Active	Inactive	Inactive	Inactive
EG-22	5050	6	Inactive	Inactive	Inactive	Inactive	Inactive
EG-23	2530	5	Inactive	Inactive	Inactive	Inactive	Inactive
EG-24	2830	5	Inactive	Inactive	Inactive	Inactive	Inactive
EG-25	340	4	Inactive	Inactive	Inactive	Inactive	Inactive
EG-26	2000	4	Inactive	Inactive	Inactive	Inactive	Inactive
Plumbagin	16	2	Inactive	Active	Inactive	Active	Inactive
Sanguinarine	778	4	Inactive	Active	Active	Active	Inactive

Table 10. Bioavailability prediction of phytoligands established in *E. ganitrus*.

Phyto-ligand	Lipophilicity (XLOGP3)	Size (MW g/mol)	Polarity (TPSA)	Insolubility [Log S (ESOL)]	Insaturation (Fraction Csp ³)	Flexibility (Num. rotatable bonds)
EG-9	3.34	368.46	74.36	−3.70	0.90	8
EG-12	4.91	206.32	20.23	−4.38	0.57	2
EG-13	3.81	276.37	43.37	−3.82	0.65	2
EG-15	4.09	222.37	20.23	−3.80	1.00	0
EG-16	4.83	273.37	52.32	−4.34	0.35	7
EG-26	1.31	209.28	29.54	−1.76	0.75	3
Plumbagin	2.29	188.18	54.37	−2.77	0.09	0
Sanguinarine	4.45	332.33	40.80	−5.24	0.15	0

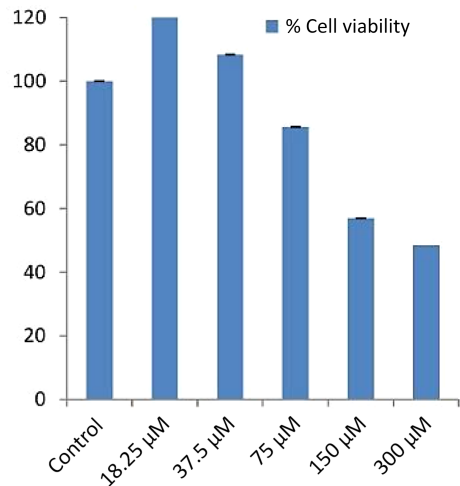


Fig. 3 IC₅₀ values of EG-13 phytochemical of *E. ganitrus* leaves against human cancer cell lines *HeLa*.

EG-9 divulged two assenting hydrogen bond interactions at the active site having amino acids of Glu96 and Lys97. In addition to that a non-classical C-H bond Vander Waals interaction was also noticed at the active site involving Arg93 residue and alkyl and pi-alkyl interactions were observed at Leu525 and Trp501 respectively. In EG-12 a conventional hydrogen bond interaction was observed at Asn538, a pi-pi T-shaped, two alkyl and a pi-alkyl interactions were observed at Tyr539, Ile522, Trp501 and Leu525 respectively. EG-13 showed one favorable hydrogen bond interaction and two hydrophobic alkyl interactions at the active site with the residue of Glu96, Leu95 and Lys97 respectively. EG-15 showed two alkyl and two pi-alkyl interactions at the active site of the residues of Leu95, Ile522, Trp501 and Tyr539 respectively. In EG-16 two conventional hydrogen bonds were observed at Leu731 and Thr716. EG-26 formed three favorable hydrogen bonds with Asp369, Asp370 and Asp371 at the active site of the receptor. Plumbagin showed a conventional hydrogen bond interaction, a pi-pi T-shaped and a carbon-hydrogen bond interaction at Tyr539, Trp501 and



Fig. 4 Bioavailability radar (pink area exhibits optimal range of particular property) for leading phytocompounds molecules. LIPO = lipophilicity as XLOGP3, SIZE = size as molecular weight, POLAR = polarity as TPSA (topological polar surface area), INSOLU = insolubility in water by log S scale, INSATU = insaturation as per fraction of carbons in the sp³ hybridization, and FLEX = flexibility as per rotatable bonds.

Ser540 respectively. Sanguinarine showed a carbon hydrogen bond, a pi-sigma, a alkyl, and a pi-alkyl interaction at the site of Glu696, Leu731, Pro769 and Pro695 respectively (Table 11). Previously it has been shown that residue at 97 could have amprospective ubiquitin acceptor position in STAT3 NH₂ terminal domain, suggesting lysine amino acid may have a significant role and location in a sumolation/ubiquitination consensus sequence^[32]. The majority of phytoligand interactions exist in the Linker domain and Transactivation domain of the STAT3.

Conclusions

All the six compounds (EG-9, EG-12, EG-13, EG-15, EG-16 and EG-26) significantly bind with STAT3. The phytochemicals epitomized good *in silico* results as reflected by their promising binding affinity, considerable inhibitory constant with optimum protein-ligand stabilization energy. Consecutively, binding signifies that phytoligands interact with STAT3 by the NH₂ terminal and boosts its transcriptional activity and interferes with the cellular proliferation process and apoptosis^[32]. Bioavailability radar and toxicological profiles of the preferred

phytoligands revealed that these compounds compel to have ample drug likeliness properties. Moreover, EG-9, EG-13, EG-15, EG-16 and EG-26 have not been explored for their anticancer potential and can be derivatized or have the probability of being used as lead compounds.

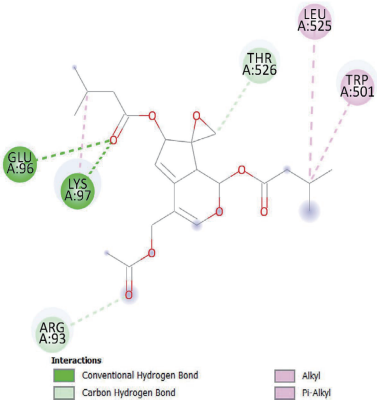
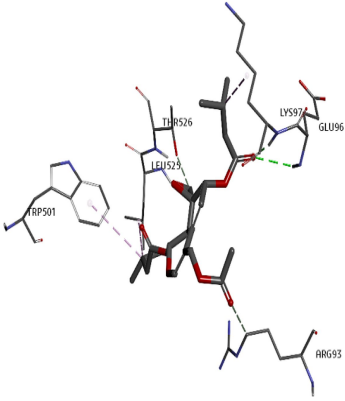
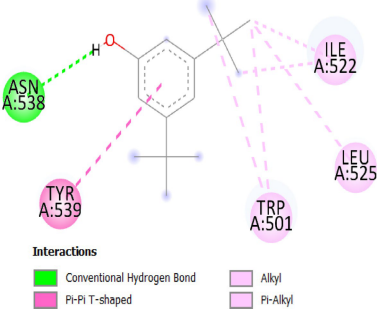
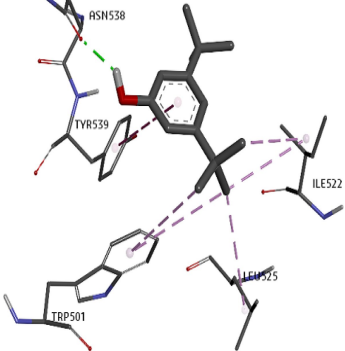
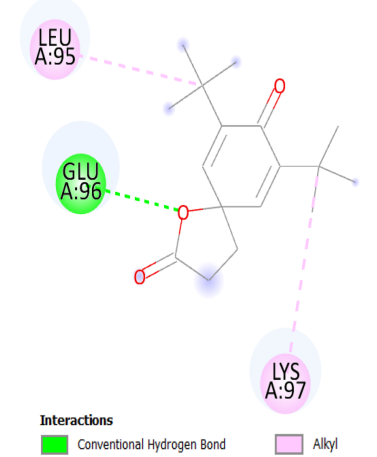
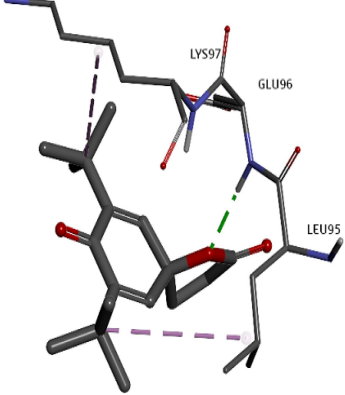
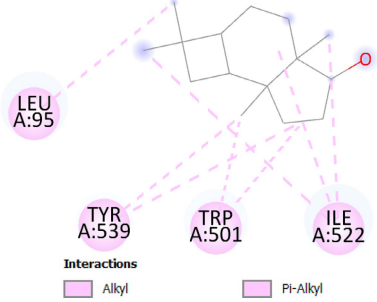
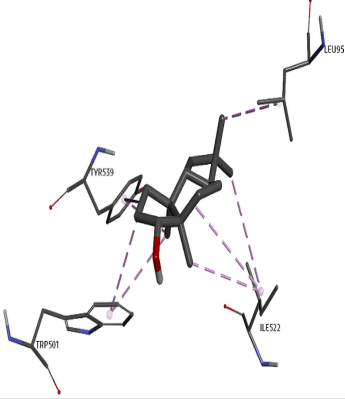
Author contributions

The authors confirm contribution to the paper as follows: study design and draft manuscript preparation (equal): Mehnaj, Bhat AR, Athar F; supervision: Athar F; experimentation and writing of manuscript: Mehnaj; characterization and editing: Bhat AR. All authors reviewed the results and approved the final version of the manuscript.

Ethical statement

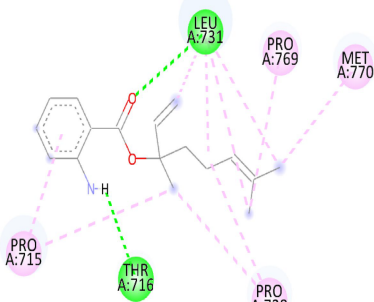
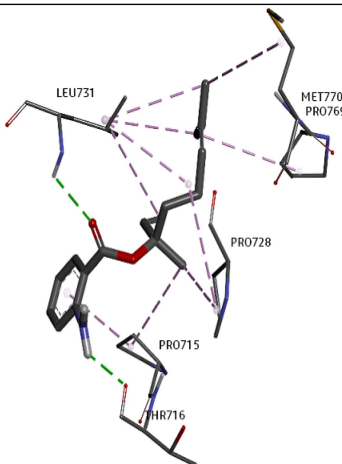
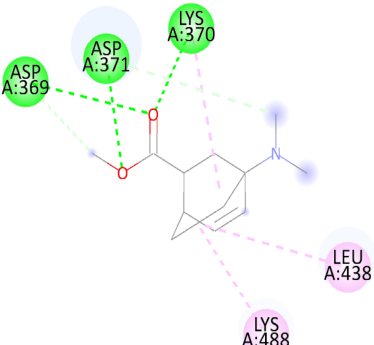
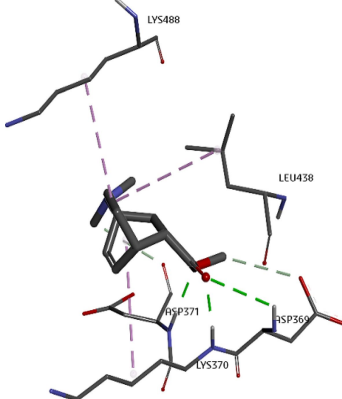
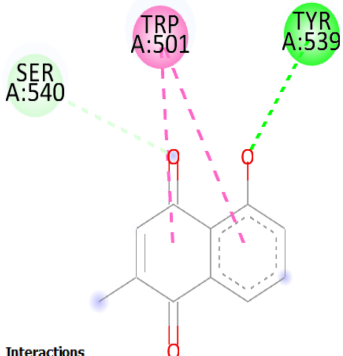
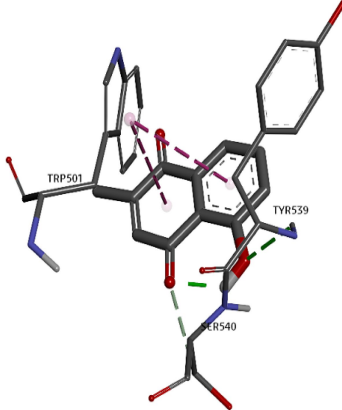
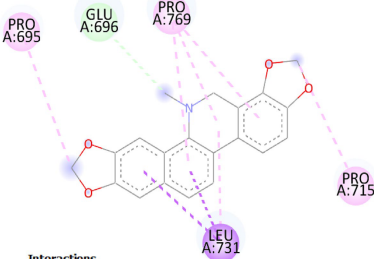
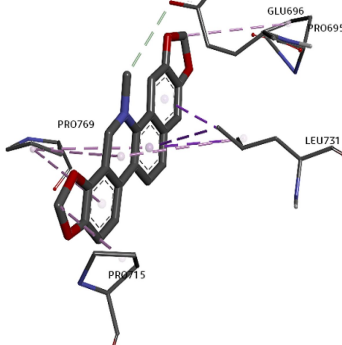
This study involved the use of established human cell lines. The cell lines used in this research were obtained from the National Centre for Cell Sciences (NCCS), Pune, India and were used in accordance with institutional and national ethical

Table 11. 2D and 3D binding interactions between the receptor 6NJS and molecules.

Phyto-ligands	2D- Binding interaction	3D- Binding interaction
EG-9 (-6.8)		
EG-12 (-6.5)		
EG-13 (-6.5)		
EG-15 (-6.5)		

(to be continued)

Table 11. (continued)

Phyto-ligands	2D- Binding interaction	3D- Binding interaction
EG-16 (-6.4)	 <p>Interactions</p> <ul style="list-style-type: none"> Conventional Hydrogen Bond Alkyl Pi-Alkyl 	
EG-26 (-5.7)	 <p>Interactions</p> <ul style="list-style-type: none"> Conventional Hydrogen Bond Carbon Hydrogen Bond Alkyl 	
Plumbagin	 <p>Interactions</p> <ul style="list-style-type: none"> Conventional Hydrogen Bond Carbon Hydrogen Bond Pi-Pi T-shaped 	
Sanguinarine	 <p>Interactions</p> <ul style="list-style-type: none"> Carbon Hydrogen Bond Pi-Sigma Alkyl Pi-Alkyl 	

standards. The cell lines have been previously published or validated, and no new human tissues were used in this study.

Data availability

The supplementary data will be made available by the authors to all upon reasonable request.

Acknowledgements

Miss Mehnaj is grateful to UGC for obtaining the non-NET fellowship allowing completion of this work.

Conflict of interest

The authors declare that they have no conflict of interest.

Dates

Received 8 December 2023; Revised 25 March 2024;
Accepted 18 April 2024; Published online 16 May 2024

References

1. Yu H, Lee H, Herrmann A, Buettner R, Jove R. 2014. Revisiting STAT3 signalling in cancer: new and unexpected biological functions. *Nature Reviews Cancer* 14:736–46
2. Zou S, Tong Q, Liu B, Huang W, Tian Y, et al. 2020. Targeting STAT3 in cancer immunotherapy. *Molecular Cancer* 19:145
3. Fan Y, Mao R, Yang J. 2013. NF- κ B and STAT3 signaling pathways collaboratively link inflammation to cancer. *Protein & Cell* 4:176–85
4. Yang X, Xu L, Yang L, Xu S. 2023. Research progress of STAT3-based dual inhibitors for cancer therapy. *Bioorganic & Medicinal Chemistry* 91:117382
5. Dong J, Cheng XD, Zhang WD, Qin JJ. 2021. Recent update on development of small-molecule STAT3 inhibitors for cancer therapy: from phosphorylation inhibition to protein degradation. *Journal of Medicinal Chemistry* 64:8884–915
6. Siveen KS, Sikka S, Surana R, Dai X, Zhang J, et al. 2014. Targeting the STAT3 signaling pathway in cancer: role of synthetic and natural inhibitors. *Biochimica et Biophysica Acta* 1845:136–54
7. Ijaz S, Akhtar N, Khan MS, Hameed A, Irfan M, et al. 2018. Plant derived anticancer agents: a green approach towards skin cancers. *Biomedicine & Pharmacotherapy* 103:1643–51
8. Salehi B, Machin L, Monzote L, Sharifi-Rad J, Ezzat SM, et al. 2020. Therapeutic potential of quercetin: new insights and perspectives for human health. *ACS Omega* 5:11849–72
9. Majolo F, de Oliveira Becker Delwing LK, Marmitt DJ, Bustamante-Filho IC, Goettvert MI. 2019. Medicinal plants and bioactive natural compounds for cancer treatment: important advances for drug discovery. *Phytochemistry Letters* 31:196–207
10. Patel B, Das S, Prakash R, Yasir M. 2010. Natural bioactive compound with anticancer potential. *International Journal of Advances in Pharmaceutical Sciences* 1:32–41
11. Mousavi SM, Hashemi SA, Behbudi G, Mazraedoust S, Omidifar N, et al. 2021. A review on health benefits of *Malva sylvestris* L. nutritional compounds for metabolites, antioxidants, and anti-inflammatory, anticancer, and antimicrobial applications. *Evidence-Based Complementary and Alternative Medicine* 2021:5548404
12. Krishna P, Kumari NR, Manisree V, Rani KS, Deepthi BVP, Sharma JVC. 2019. Medicinal benefits of *Elaeocarpus Ganitrus* (Rudraksha) - A divine herb. *World Journal of Pharmaceutical Research* 8:552–65
13. Mahajanakatti AB, Deepak TS, Achar RR, Pradeep S, Prasad SK, et al. 2022. Nanoconjugate synthesis of *Elaeocarpus ganitrus* and the assessment of its antimicrobial and antiproliferative properties. *Molecules* 27:2442
14. Das PK. 2015. Phytochemical screening of methanolic extracts of different parts of rudraksh plant (*Elaeocarpus ganitrus*). *Journal of Biological Sciences* 15:111–12
15. Motallebi M, Bhia M, Rajani HF, Bhia I, Tabarraei H, et al. 2022. Naringenin: a potential flavonoid phytochemical for cancer therapy. *Life Sciences* 305:120752
16. Zhang Y, Liu X, Ruan J, Zhuang X, Zhang X, et al. 2020. Phytochemicals of garlic: promising candidates for cancer therapy. *Biomedicine & Pharmacotherapy* 123:109730
17. Fulda S, Debatin KM. 2006. Resveratrol modulation of signal transduction in apoptosis and cell survival: a mini-review. *Cancer Detection and Prevention* 30:217–23
18. Ahmad K, Bhat AR, Athar F. 2017. Pharmacokinetic evaluation of *Callistemon viminalis* derived natural compounds as targeted inhibitors against δ -opioid receptor and farnesyl transferase. *Letters in Drug Design & Discovery* 14:488–99
19. Sudradjat SE, Timotius KH. 2022. Pharmacological properties and phytochemical components of *Elaeocarpus*: a comparative study. *Phytomedicine Plus* 2:100365
20. Kumar TS, Shanmugam S, Palvannan T, Bharathi Kumar VM. 2008. Evaluation of antioxidant properties of *Elaeocarpus ganitrus* roxb. leaves. *Iranian Journal of Pharmaceutical Research* 7(3):211–15
21. Sultana B, Anwar F, Ashraf M. 2009. Effect of extraction solvent/technique on the antioxidant activity of selected medicinal plant extracts. *Molecules* 14:2167–80
22. Ozigis HO, Olaifa KA, Agbeja AO, Asabia LO, Akindolu DR, et al. 2023. Qualitative phytochemical analysis of leave and stem bark of *Zanthoxylum zanthoxyloides* and *Zanthoxylum gillettii*. *Journal of Chemical Society of Nigeria* 48(3):891
23. Dhivya R, Jaividhya P, Riyasdeen A, Palaniandavar M, Mathan G, et al. 2015. *In vitro* antiproliferative and apoptosis-inducing properties of a mononuclear copper(II) complex with dppz ligand, in two genotypically different breast cancer cell lines. *BioMetals* 28:929–43
24. Daina A, Michielin O, Zoete V. 2017. SwissADME: a free web tool to evaluate pharmacokinetics, drug-likeness and medicinal chemistry friendliness of small molecules. *Scientific Reports* 7:42717
25. Lipinski CA. 2004. Lead- and drug-like compounds: the rule-of-five revolution. *Drug Discovery Today Technologies* 1:337–41
26. Khan A, Mohammad T, Shamsi A, Hussain A, Alajmi MF, et al. 2022. Identification of plant-based hexokinase 2 inhibitors: combined molecular docking and dynamics simulation studies. *Journal of Biomolecular Structure & Dynamics* 40:10319–31
27. Banerjee P, Eckert AO, Schrey AK, Preissner R. 2018. ProTox-II: a webserver for the prediction of toxicity of chemicals. *Nucleic Acids Research* 46:W257–W263
28. Beg A, Khan FI, Lobb KA, Islam A, Ahmad F, et al. 2019. High throughput screening, docking, and molecular dynamics studies to identify potential inhibitors of human calcium/calmodulin-dependent protein kinase IV. *Journal of Biomolecular Structure & Dynamics* 37:2179–92
29. Tsaïoun Katya, Kates SA. (Eds) 2011. *ADMET for medicinal chemists: a practical guide*. Hoboken, New Jersey (simultaneously in Canada): John Wiley & Sons. <https://doi.org/10.1002/9780470915110>
30. Onawole AT, Sulaiman KO, Adegoke RO, Kolapo TU. 2017. Identification of potential inhibitors against the Zika virus using consensus scoring. *Journal of Molecular Graphics & Modelling* 73:54–61
31. Siramshetty VB, Nickel J, Omieczynski C, Gohlke BO, Drwal MN, et al. 2016. WITHDRAWN—a resource for withdrawn and discontinued drugs. *Nucleic Acids Research* 44:D1080–D1086
32. Ray S, Zhao Y, Jamaluddin M, Edeh CB, Lee C, et al. 2014. Inducible STAT3 NH2 terminal mono-ubiquitination promotes BRD4 complex formation to regulate apoptosis. *Cellular Signalling* 26:1445–55



Copyright: © 2024 by the author(s). Published by Maximum Academic Press, Fayetteville, GA. This article is an open access article distributed under Creative Commons Attribution License (CC BY 4.0), visit <https://creativecommons.org/licenses/by/4.0/>.